

Bathymetry Estimation from Satellite Altimeter-Derived Gravity Data

Ljerka Vrdoljak and Tomislav Bašić

Abstract

Bathymetry underpins all marine and ocean research. It is common knowledge that there is a global deficit of high-resolution bathymetry based on modern acoustic techniques. Satellite altimetry enabled modeling of the global seafloor topography and revealed new morphological features in the unmapped areas of the oceans and seas. This chapter gives an overview of the physical problem and different approaches to estimating the bathymetry from satellite altimeter-derived gravity data. Characteristics of recent versions of frequently used global bathymetry models are presented. Moreover, this chapter demonstrates the possibility of regional bathymetry modeling by the gravity-geologic method in the Adriatic Sea.

Keywords: bathymetry mapping, global bathymetry grids, gravity anomalies, gravity-geologic method, regional bathymetry modeling

1. Introduction

Bathymetry is an important input parameter or a frame that supports all marine research. Although there are global and regional initiatives to improve our understanding of seafloor topography [1–3], less than 25% of the world's seas have been mapped with high resolution that is able to identify features of a few tens of meters in size [1]. Current global seafloor topography is estimated from altimeter data and augmented with available grids from a variety of techniques, mainly shipborne depth soundings [1, 2, 4–7]. As compared to modern acoustic techniques, bathymetry derived from altimetry has a coarse spatial resolution [8]. However, the data from altimeter missions enabled revealing of buried and unmapped features of global seafloor topography [4, 9]. Altimeter data supplemented the sparse shipborne soundings and improved our knowledge of the seafloor topography by bathymetry inversion from altimeter-derived gravity anomalies. Global marine gravity grids formed from high-density altimeter data (e.g. [10, 11]) and digital data bases of shipborne soundings (e.g. [10]) enabled estimation of global seafloor topography [11].

This chapter gives an overview of the relationship between the topography of the seafloor and gravity. Diverse approaches to estimate the bathymetry from altimeter-derived gravity data, in space and frequency domain, are briefly presented.

Characteristics of frequently used global bathymetry models are depicted. Moreover, the chapter demonstrated the possibility of regional bathymetry modeling by the gravity-geologic method (GGM) in the Adriatic Sea. The estimated bathymetry grid was compared to global grids in the study area, and their quality was assessed as compared to chart soundings.

2. The relationship between depth and gravity

The depth variations of the seafloor can be observed as height variations of mass elements of the density $\Delta\rho$ which is the contrast between the density of the seafloor ρ_c and seawater ρ_w [12]. The result of the seafloor topography variation is the disturbance in the local gravity field.

The disturbing potential $T(r)$ due to mass element of the volume V and density $\Delta\rho$ is [12]:

$$T(r) = G\Delta\rho \int_V \frac{dV}{|r - r'|} \quad (1)$$

where G is the gravitational constant, r is the coordinate vector of location, and r' is the coordinate vector of the center of the mass element.

The geoid undulation N is related to the disturbing potential T by Brun's formula [11, 12]:

$$N \cong \frac{1}{g_0} T \quad (2)$$

where g_0 is the average acceleration of gravity regarding the geodetic latitude.

The gravity anomaly Δg is the vertical derivate of the disturbing potential [11, 12]:

$$\Delta g = -\frac{\partial T}{\partial z} \quad (3)$$

The east and the north component of vertical deflection represent the slope of the geoid in x and y direction:

$$\eta = -\frac{1}{g_0} \frac{\partial T}{\partial x}, \xi = -\frac{1}{g_0} \frac{\partial T}{\partial y} \quad (4)$$

Laplace's equation links these quantities together [11, 12]:

$$\frac{\partial \eta}{\partial x} + \frac{\partial \xi}{\partial y} = -\frac{\partial \Delta g}{\partial z} \quad (5)$$

Disaggregating of the computation area in Eq. (1) into discretized elements of surface $\Delta\Omega(r')$ and regarding the Eq. (2), topography undulation $N(r)$ is given by [12]:

$$N(r) = \frac{G}{g_0} \Delta\rho \sum_{r'} \Delta\Omega(r') \int_{z_b}^{z_t} \frac{dz}{|r - r'|} \quad (6)$$

where z_b i z_t are depth on the bottom and top of the mass element.

In spectral domain, relationship between topography of the seafloor and gravity anomalies is [13]:

$$F[\Delta g] = 2\pi G(\rho_c - \rho_w)e^{-2\pi kd} \sum_{n=1}^{\infty} \frac{(2\pi k)^{n-1}}{n!} F[h^n] \quad (7)$$

where $F[]$ is the two-dimensional Fourier transform operator, k is the wave number; $k = \sqrt{k_x^2 + k_y^2}$ where $k_x=1/\lambda_x$, a $k_y=1/\lambda_y$, λ_x i λ_y are wavelengths at x and y direction, and h is depth of the seafloor located at the mean sea depth d .

There are several inverse approaches to model topography of the seafloor from altimeter-derived gravity anomalies [12]

In this study, two commonly used approaches are reviewed, Smith and Sandwell (S&S) in frequency domain and gravity-geologic method (GGM) in space domain.

2.1 Smith and Sandwell approach (S&S)

Smith and Sandwell [4, 9, 11] suggested that a correlation between variations in altimeter-derived gravity anomalies and topography of the seafloor can be found in the wavelength band of 15–200 km. If variations in seafloor undulations are much smaller than mean sea depth, Eq. (7) can be limited to the first term [11]:

$$G(k) = 2\pi G(\Delta\rho)e^{-2\pi kd}H(k) = Z(k)H(k) \quad (8)$$

$$H(k) = Z^{-1}(k)G(k) \quad (9)$$

where $G(k)$ is a Fourier transform of the gravity anomalies, $H(k)$ is a Fourier transform of the seafloor topography, and $Z(k)$ is the isotropic transfer or the admittance function.

The main steps in the S&S approach are as follows [4, 9, 11]:

The base bathymetry grid in frequency domain $H_B(k)$ is separated into low-pass (long-wavelength) bathymetry $H_L(k)$ and high-pass (short-wavelength) bathymetry $H_S(k)$ components using a Gaussian filter.

Gravity anomalies in the frequency domain $G(k)$ are band-pass filtered and downward continued using the Wiener filter $W(k)$ to stabilize the procedure:

$$G_{BP}(k) = G(k) W(k) e^{2\pi kd} \quad (10)$$

The Wiener filter is composed of high-pass filter $W_1(k)$ and low-pass filter $W_2(k)$ whose original forms are defined by Smith and Sandwell [4].

The band-passed filtered bathymetry $H_{BP}(k)$ is obtained by applying the filter to base bathymetry grid in the frequency domain.

According to the admittance theory [14], the relationship between gravity and topography is linear, so topography can be inverted from gravity by simply multiplying with theoretical topography/ratio scaling factor $S_T = (2\pi G\Delta\rho)^{-1}$ [12]. Instead of using the theoretical value, in overlapping area, a robust regression analyse is performed between band-passed bathymetry $H_{BP}(k)$ and band-passed gravity anomalies $G_{BP}(k)$ to estimate the topography/ratio scaling S .

The total predicted bathymetry by S&S approach in the space domain $d_p(x)$ is

$$d_p(x) = d_L(x) + S g(x) + d_S(x) \quad (11)$$

where $d_L(x)$ and $d_S(x)$ are the spatial domain of the low-passed bathymetry $H_L(k)$ and high-passed bathymetry $H_S(k)$, respectively, and $g(x)$ is a spatial domain of band-passed gravity $G_{BP}(k)$.

2.2 Gravity-geologic method (GGM)

Although the gravity-geologic method (GGM) was originally used to determine the depth of a glacial sediment above the bedrock [15], it has been adopted and utilized in recent studies to estimate the regional bathymetry from altimetry [16–20].

The observed free-air gravity anomalies at the sea surface Δg can be separated to the referent, long-wavelength gravity Δg_{long} caused by the distribution of masses deep inside the Earth's body and the residual, short-wavelength gravity field Δg_{short} caused by the distribution of masses above the datum D . Datum D is usually determined as the deepest depth.

The GGM calculates the residual field from a Bouguer slab formula using the control soundings d_j :

$$\Delta g_{short}(j) = 2\pi G \Delta \rho (d_j - D) \quad (12)$$

where G is the gravitational constant and $\Delta \rho$ is the density contrast between seafloor and seawater.

The long-wavelength gravity field in the known points $\Delta g_{long}(j)$ is determined by the simple subtraction:

$$\Delta g_{long}(j) = \Delta g(j) - \Delta g_{short}(j) \quad (13)$$

The long-wavelength gravity is then interpolated to the unknown i -th points from the known $\Delta g_{long}(j)$ at known j -th points. The short-wavelength gravity $\Delta g_{short}(i)$ at unknown i -th points is calculated by subtracting the long-wavelength gravity $\Delta g_{long}(i)$ from the observed gravity $\Delta g(i)$:

$$\Delta g_{short}(i) = \Delta g(i) - \Delta g_{long}(i) \quad (14)$$

Depth at the unknown points d_i is determined by simple inversion of the Eq. (12):

$$d_i = \frac{\Delta g_{short}(i)}{2\pi G \Delta \rho} + D \quad (15)$$

3. Global bathymetry models

Global bathymetry models have been constructed based on satellite altimetry, employing different data and techniques. **Table 1** presents a summary of attributes of recognized and frequently used global bathymetry models (recent version): (1) DTU10BAT (Bathymetry model from Space Institute of the Technical University of Denmark) [26], (2) ETOPO 1 (National Oceanic and Atmospheric Administration ETOPO 1 Arc-Minute Global Relief Model) [7], (3) GEBCO 2021 (The General Bathymetric Chart of the Ocean) [6], (4) SRTM 15+ v2.3 (Shuttle Radar Topography

DBM	DTU10BAT	ETOPO 1	GEBCO 2021	SRTM15+ v2.3	SS v20.1
Grid Spacing	1'-2' (Equator)	1'	15"	15"	1'
Release Year	2010	2009	2021	2021	2020
Based on	Altimeter-derived gravity DTU10 and ship depth soundings	±80° latitude 2 arc min SS grid (2008)	SRTM15+ v2.2 augmented with additional bathymetry	Altimeter-derived gravity and ship depth soundings	Altimeter-derived gravity and ship depth soundings
Website	[21]	[22]	[23]	[24]	[25]

Table 1.
Global bathymetry models relying on satellite altimetry.

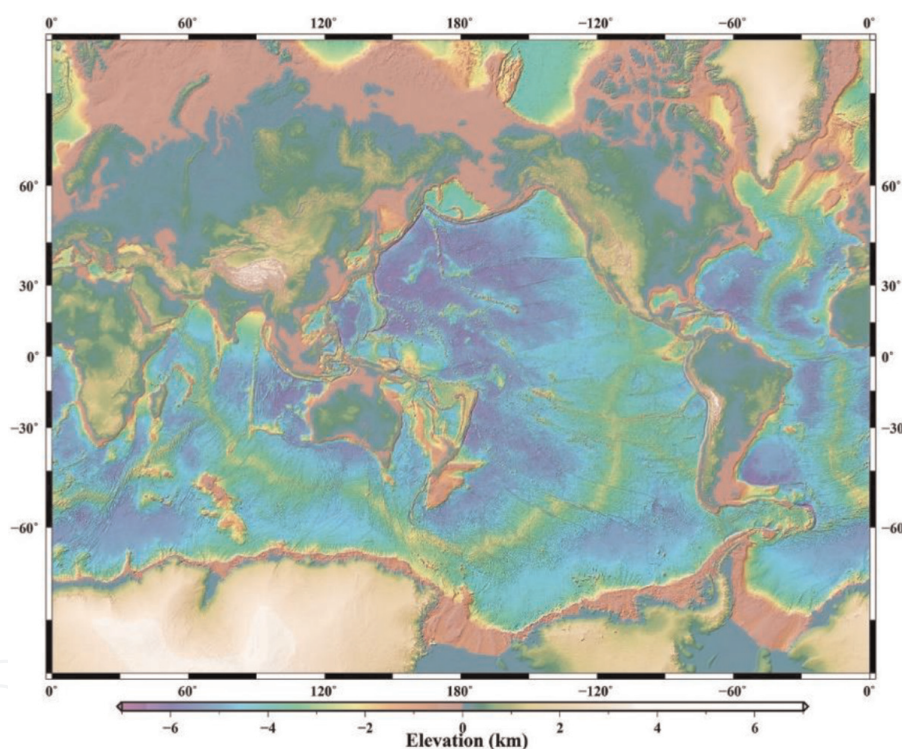


Figure 1.
Global bathymetry and topography at 15 arc seconds [5].

Mission: Global Bathymetry and Topography at 15 arc seconds) [5], and (5) SS v20.1 (Global topography from Scripps Institution of Oceanography) [4].

Global seafloor topography (**Figure 1**) relies on bathymetry estimated from altimeter-derived gravity anomalies, employing the S&S approach in the frequency domain adjusted for digital data processing. The base bathymetry layer is afterwards augmented by bathymetric data from other in situ or remote sensing techniques and existing composite bathymetry grids.

Several studies evaluated and compared available bathymetry grids on a global and regional scale [27–30]. Differences between grids resulted from different density, distribution and accuracy of the input bathymetry, grid misregistration, data smoothing, and integration of different datasets to form the global grid [27, 30]. Quality of

depth estimated from the altimeter derived gravity is related to limitations of the altimeter technology, causing robust bathymetry due to the noise in the solution [27, 29] and large discrepancies in coastal areas [30]. SS global bathymetry model provided a base bathymetry layer for most of global and regional bathymetry solutions. SS model reflects state of the art in marine gravity modeling [31]. Combined with a large database of shipborne surveys at Scripps Institution of Oceanography, the SS model is continuously upgraded and generally considered to be a reliable and up-to-date bathymetry source [27]. However, an uneven distribution of sparse in situ bathymetric data can result in large depth anomalies in the inversion of the seafloor topography. On a global scale, depth uncertainty can be expected to be less than 100 meters in deep ocean areas and greater than 100 meters between the shoreline and the continental rise [5, 28].

4. Regional bathymetry modeling: A case study of Adriatic Sea

There is an ongoing effort by the scientific community to improve bathymetry solutions on global and regional scale [1, 2]. Base bathymetry estimated from altimeter-derived gravity is augmented with high-quality survey grids or composite bathymetry products. The GGM method has been successfully utilized for regional bathymetry modeling in different marine regions [16–20, 32, 33]. The difference between the quality of models derived from the GGM and the S&S approach is negligible, as it is more dependent on the availability of the shipborne soundings [33]. The GGM method has an algorithm in the spatial domain, so there is no need for transformation to a frequency domain, but the accuracy of the method depends on the density and distribution of shipborne soundings, and the estimation of a density contrast between the seafloor and seawater [33].

In this study, a 1/16' by 1/16' bathymetry model of the Adriatic was constructed by the GGM method. The base model was augmented by the *in situ* soundings from EMODnet network and nautical charts. The model was compared to the global solutions listed in Par. 3, and the quality of the models was estimated regarding chart soundings.

4.1 Study area and datasets

4.1.1 Study area

The Adriatic Sea (12° 3' – 20° 1' E, 39° 44' - 45° 48' N) is the most northern part of the Mediterranean Sea connected to the Ionian Sea via the Strait of Otranto. Limits of the Adriatic Sea and land mask were adopted from IHO and the Flanders Institute [34, 35]. The Adriatic Sea is a shallow sea with a median depth of 100 meters [36]. By bathymetry, the Adriatic is divided into three sub-basins: the shallowest North sub-basin, the transitional zone of the Middle sub-basin, and the South sub-basin that comprises the South Adriatic Pitt, the deepest part of the Adriatic with depths extending under 1200 meters (**Figure 2**) [36].

4.1.2 Altimeter-derived gravity anomalies

This study explores the possibility of inverting bathymetry from altimeter-derived gravity anomalies by the GGM method in the Adriatic Sea. Models of free-air gravity

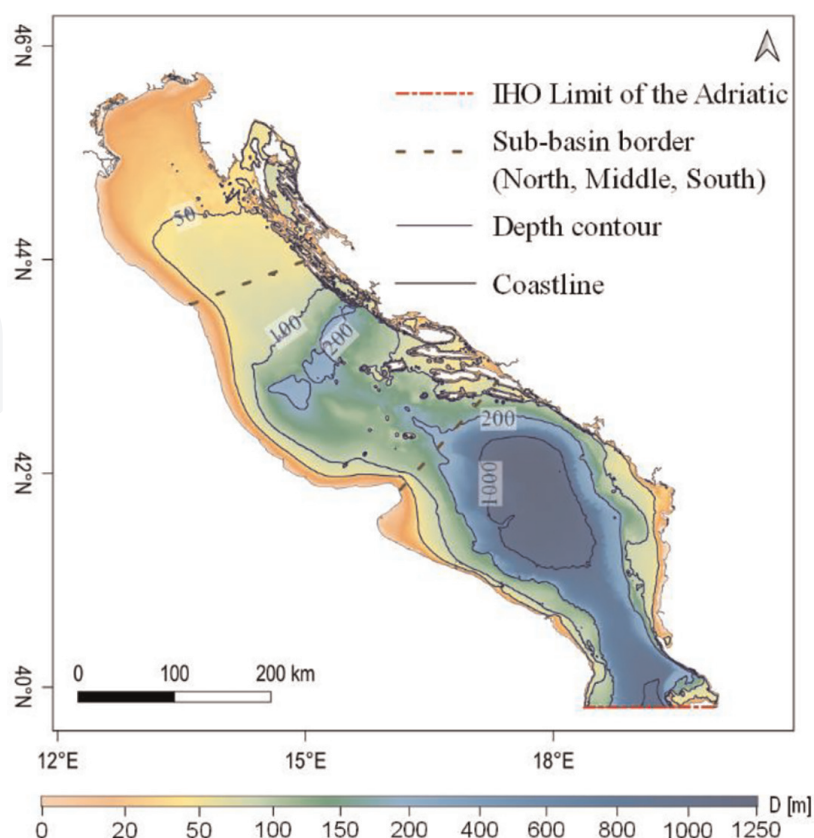


Figure 2.
 Adriatic Sea. (Bathymetry source [6]).

Δg	DTU10 [10^{-5} ms^{-2}]	SS v.29.1 [10^{-5} ms^{-2}]
MIN	-116.22	-135.40
MAX	115.14	129.80
MEAN	-15.20	-15.65
σ	35.52	36.90

Table 2.
 Statistic of gravity anomalies in the Adriatic from DTU 10 and SS v 29.1 models: minimum (MIN), maximum (MAX), mean and standard deviation (σ).

anomalies from the Technical University of Denmark, DTU10 model [26], and from Scripps Institution of Oceanography, SS v. 29.1 [31] were used. General statistics of models in the study area is presented in **Table 2**.

The current accuracy of gravity anomalies derived from altimeter data is around $2 \times 10^{-5} \text{ ms}^{-2}$ [31]. As presented in **Figure 3c**, the largest differences between models ($>40 \times 10^{-5} \text{ ms}^{-2}$) were along well-indented eastern Adriatic coast.

4.1.3 Control and check soundings

Control bathymetry was composed from EMODnet 2020 bathymetry [2] in the western Adriatic, GEBCO One Minute Grid [37] in the south-eastern Adriatic and soundings from nautical charts in the eastern Adriatic (**Figure 4a**). Control bathymetry,

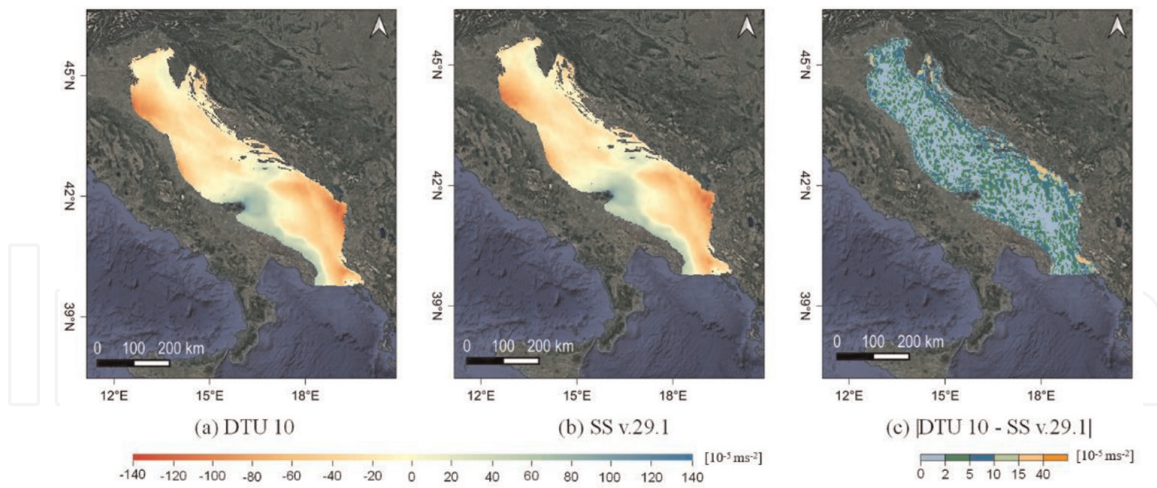


Figure 3. Free-air gravity anomalies over Adriatic Sea: (a) DTU10 gravity anomaly, (b) SS v29.1 gravity anomaly, and (c) absolute difference between models [26, 31].

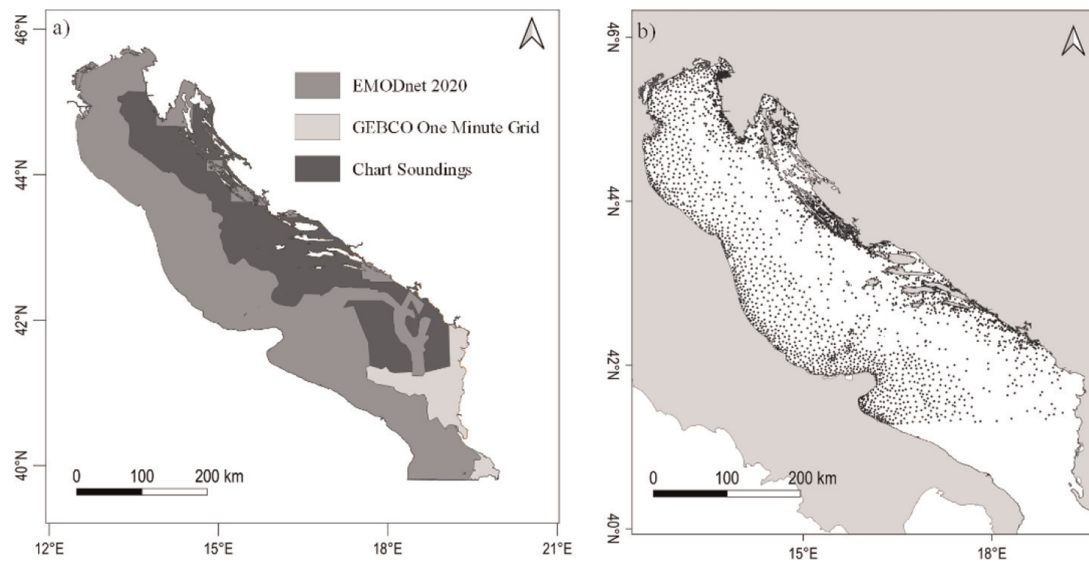


Figure 4. (a) Control soundings and (b) check soundings.

needed for accurate modeling of the referent gravity field, consisted of 45 666 depths. Over 3500 soundings from nautical charts were used as check soundings needed for the estimation of a density contrast and quality control (Figure 4b). The quality of control and check soundings was estimated to be better than $2 + 0.05\%$ depth meter [2].

4.2 Methodology

4.2.1 Bathymetric recipe

Bathymetry was calculated in three steps:

1. The first step was constructing the base bathymetric layer. The 1 arc-minute base bathymetric grid was estimated from gravity anomalies using the gravity-geologic method (GGM) (Par. 2. 2).

2. Differences between the control soundings and base bathymetry were derived. Gaps between points, at a distance larger than 1 arc minute from a point, were filled with zero values to prevent the generation of artificial morphology [5]. Differences were gridded to a model with a 1/16 arc-minute grid spacing.
3. The base bathymetry layer was re-interpolated to 1/16 arc-minute grid spacing using a bilinear interpolation. The final bathymetry model resulted in adding the differences to the re-interpolated base bathymetry.

4.2.2 Comparison and quality assessment of bathymetric grid

For pixel-to-pixel comparison between the calculated model of the Adriatic Sea and available global grids in the study area, global grids were resampled to a grid spacing of 1/16 arc-minute by bilinear interpolation. Absolute differences between the calculated digital bathymetry model (DBM) and global models in identical points were calculated and analyzed.

Residuals between check soundings and model were taken as a measure of model accuracy. With the most widely used measure for quality assessment root mean square error (RMSE), a normalized root mean square error (NRMSE) was calculated in different depth ranges.

4.3 Result

4.3.1 Digital bathymetry model of the Adriatic Sea GGM+ DBM

Bathymetry of the Adriatic Sea was estimated from altimeter-derived gravity anomalies by the GGM method, using a theoretical density contrast between the seafloor topography and the seawater of 1670 kg m^{-3} . The bathymetric model inverted from DTU 10 gravity anomalies has the RMSE of 25.41 m, while bathymetry estimated from SS v 29.1 gravity anomalies has the RMSE of 30.05 m. The tuning density contrast, which minimized the RMSE of the predicted bathymetry, was estimated by a trade-off diagram. As shown in **Figure 5**, a density contrast higher than 10^4 kg m^{-3} stabilized the trade-off diagram around RMSE of 14 m and a correlation (r_p) of 99.60%.

Tuning density contrast of 15000 kg m^{-3} was chosen to predict bathymetry by the GGM method in the Adriatic Sea. The digital bathymetry model (DBM) derived from DTU10 gravity anomalies (DTU10 DBM₁₅) had the RMSE of 13.80 m. The RMSE of a

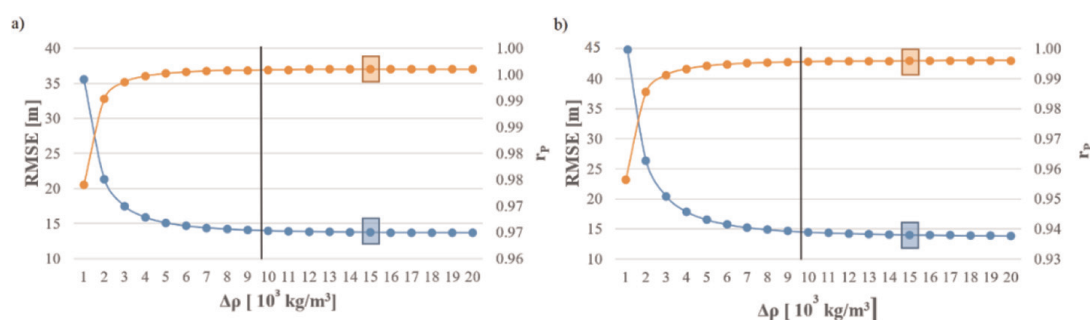


Figure 5. Trade-off diagram for selecting a tuning density contrast in the study area for bathymetry modeling by GGM method (a) from DTU 10 gravity anomalies and (b) from SS v.29.1 gravity anomalies.

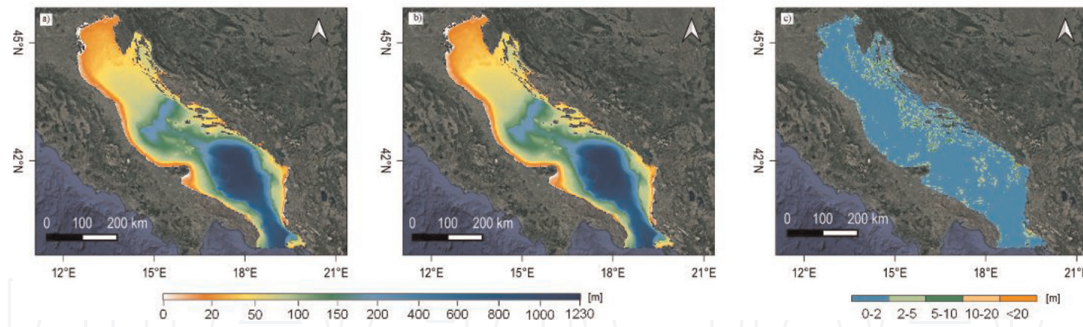


Figure 6. Digital bathymetry models estimated from altimeter-derived gravity anomalies: (a) DTU10 DBM₁₅, (b) SS DBM₁₅, and (c) absolute differences between models.

DBM	Depth[m]			
	Max	Mean	Median	σ
DTU 10 DBM ₁₅	1225	250	100	342
SS DBM ₁₅	1224	250	100	342

Table 3.

Summary statistics of DTU10 DBM₁₅ and SS DBM₁₅ digital bathymetric models (DBM): maximum depth (Max), mean depth (Mean), median depth (Median), and standard deviation of depth (σ).

DBM derived from SS v 29.1 gravity anomalies (SS DBM₁₅) was 14.0 m. **Figure 6** represents 1 arc-minute DBMs of the Adriatic referring to the Mean Sea Level (MSL). DBMs were derived from DTU10 and SS v 29.1 gravity anomalies by the GGM method using the tuning density contrast of $15\,000\text{ kgm}^{-3}$.

Summary statistics of DTU10 DBM₁₅ and SS DBM₁₅ models over study area is presented in **Table 3**.

DTU10 DBM₁₅ and SS DBM₁₅ had a high degree of correspondence due to the equal tuning density contrast for bathymetry inversion by the GGM method. The largest discrepancies were in the coastal area along the eastern coast (**Figure 6c**). That resulted from the differences between input gravity models.

DTU10 DBM₁₅ bathymetric model has a slightly lower RMSE compared to SS DBM₁₅. Therefore, it was chosen as a base bathymetric layer to compute an enhanced bathymetry model of the Adriatic Sea (GGM+ DBM). If possible, pixel values were reset to the value of directly observed bathymetry. A modified Remove-Restore procedure was applied [5]. GGM+ DBM with 1/16 arc-minute grid spacing was enhanced by the EMODnet 2020 grid in the Western Adriatic, and in the Eastern Adriatic it was augmented with chart soundings (**Figure 7**).

In terms of residuals between the check soundings and predicted depth, there is a slight improvement of the RMSE of 5% (RMSE = 13 m).

4.3.2 Comparison with global bathymetric models in the Adriatic Sea

In this section, the GGM+ DBM was compared with data from global bathymetric grids in the Adriatic Sea: DTU10BAT [26], ETOPO 1 [7], GEBCO 2021 [6], SRTM 15+ v2.3 [5], and SS v20.1 [4]. Absolute differences between the GGM+ DBM and global grids at mutual 15 arc seconds resolution are presented in **Figure 8**.

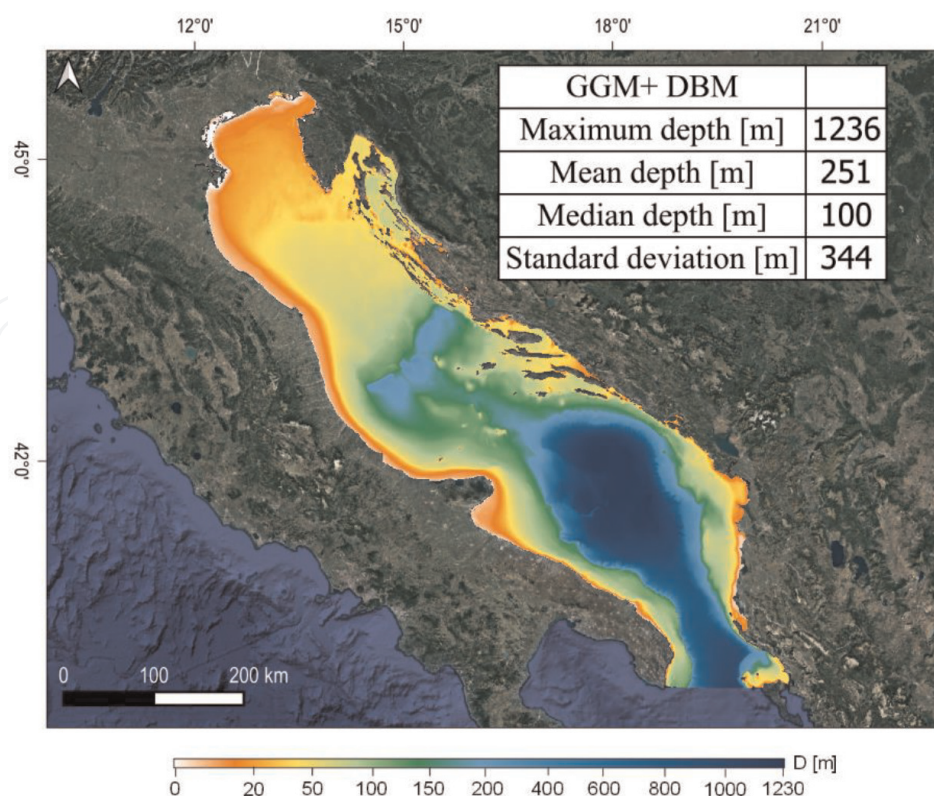


Figure 7.
 Bathymetric model of the Adriatic Sea GGM+ DBM.

Statistics of absolute differences between GGM+ DBM and analyzed bathymetry models over study area are given in **Table 4**.

As compared to the GGM+ DBM, the DTU10BAT, and the ETOPO 1, bathymetric models were the models with the greatest discrepancies throughout the study area, especially along the eastern coast. SS v20.1 and SRTM15+ v2.3 showed similar spatial distribution of absolute differences. GEBCO 2021 DBM had the best alignment with the GGM+ DBM over the study area with the median absolute difference of 2 meters. This is less than 1% of the average depth of the Adriatic Sea. Generally, absolute differences along the eastern well-indented coast are larger than along the western coast for all the models. The level of similarity and homogeneity between models is highly influenced by the input data and methodology upon which the grids were constructed, especially the distribution and quality of the input bathymetry.

4.3.3 Quality assessment of bathymetric models in Adriatic Sea

Depth of the analyzed DBMs were compared to the check soundings. The RMSE of the DBMs in the Adriatic Sea is presented in **Table 5**.

More recent digital bathymetric models (GEBCO 2021, GGM+ DBM, SS v20.1, and SRTM 15+ v2.3) showed better accuracy than the older versions (DTU10BAT and ETOPO1). Recent versions were derived from up-to-date altimetry data and/or more dense bathymetry data.

Quality of the DBMs was compared in different depth ranges: 0–20 m, 20–50 m, 50–100 m, 100–200 m, and deeper than 200 m (**Figure 9**). The NRMSE was chosen as a quality measure.

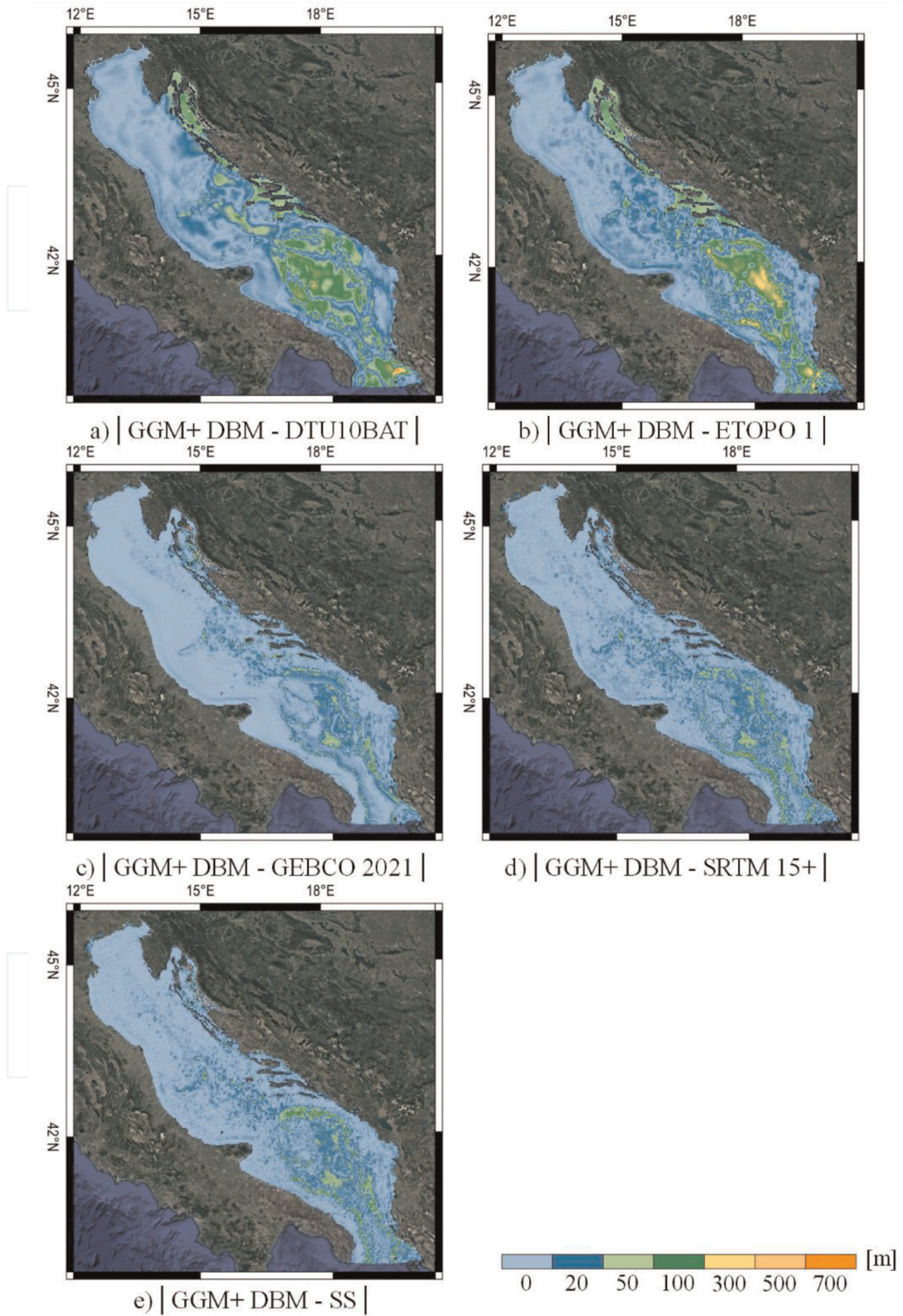


Figure 8. Absolute difference between GGM+ DBM and (a) DTU₁₀BAT, (b) ETOPO₁, (c) GEBCO 2021, (d) SRTM 15+, and (e) SS in the Adriatic.

$ \Delta D $	MAX [m]	MEAN [m]	σ [m]	MEDIAN [m]
GGM+ DBM - DTU10BAT	686	26	39	8
GGM+ DBM - ETOPO 1	482	26	47	7
GGM+ DBM - GEBCO 2021	214	7	12	2
GGM+ DBM - SRTM15+ v2.3	562	9	18	4
GGM+ DBM - SS v20.1	585	10	19	3

Table 4.
 Statistics of absolute differences between GGM+ DBM and global grids in the Adriatic.

DBM	RMSE [m]
DTU10BAT	36
ETOPO1	36
GEBCO 2021	17
SRTM15+ v2.3	11
SS v20.1	16
GGM+ DBM	13

Table 5.
 Quality of bathymetric models in the Adriatic Sea.

Generally, the lowest accuracy of the predicted depth was in the shallowest depth range, up to 20 meters deep. The error was larger than 100% of the depth for the SS v20.1 DBM. Lower accuracy is the result of the coarse resolution of the models and the limitation of altimeter technology in coastal areas. As presented in **Figure 9**, bathymetry estimated from altimeter-derived gravity anomalies had better agreement with seafloor topography in deeper seas. In marine areas in the Adriatic Sea that are over 200 meters deep, the accuracy of bathymetric estimation was up to 10% of the depth.

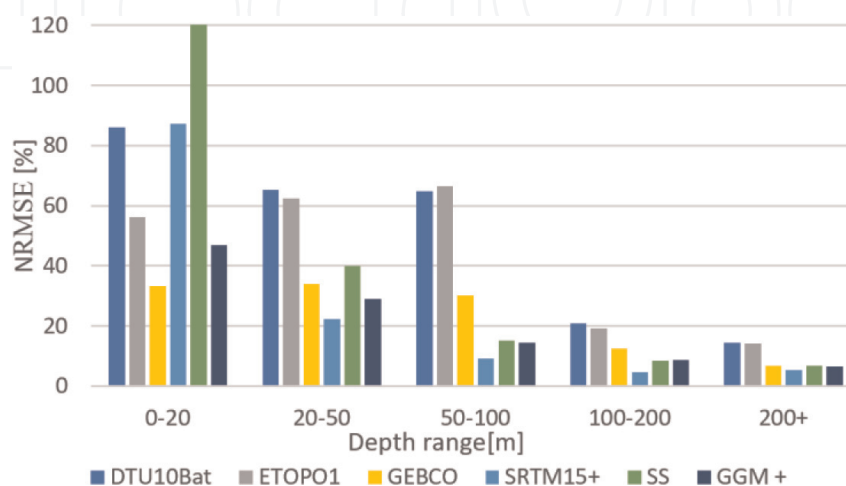


Figure 9.
 Quality of bathymetric models in the Adriatic Sea in different depth ranges.

5. Conclusion

Altimeter technology enhanced our knowledge of the seafloor topography and revealed morphological features of the unmapped ocean areas. Widely used global bathymetry models are calculated by the Smith and Sandwell approach (S&S) in the frequency domain. This chapter presented the possibility of regional bathymetry modeling by the gravity-geologic method (GGM) in the space domain with a simpler algorithm, higher resolution, and satisfactory quality as compared to global solutions.

The digital bathymetry model of the Adriatic Sea with 1/16 arc-minute grid spacing (GGM+ DBM) was estimated from the DTU10 model of marine gravity anomalies by the GGM method. Density contrast between seafloor and seawater of $15\,000\text{ kgm}^{-3}$, selected from the trade-off diagram, had minimized the root mean square error (RMSE). The model was augmented by depth soundings from the EMODnet grid in the West Adriatic and nautical charts in the East Adriatic. GGM+ DBM is well adjusted to the topography of the Adriatic Sea, with the RMSE of 13 m.

As compared to modern shipborne bathymetric surveys, bathymetry estimated from altimetry has a coarse spatial resolution and lower accuracy, especially in coastal areas. The greatest discrepancies between the global grids and the GGM+ DBM are along the eastern Adriatic coast due to altimetry limitation and diverse input bathymetry. As compared to chart soundings, all models had the lowest accuracy in the coastal area shallower than 20 m. The quality increased up to 10% of the depth in the deepest parts of the Adriatic. Limitations of the bathymetry estimated from altimetry can be overcome by more available high-quality bathymetry in important coastal areas.

Author details


Ljerka Vrdoljak^{1*} and Tomislav Bašić²

1 Hydrographic Institute of the Republic of Croatia, Split, Croatia

2 University of Zagreb, Croatia

*Address all correspondence to: ljerka.vrdoljak@hhi.hr

IntechOpen

© 2022 The Author(s). Licensee IntechOpen. This chapter is distributed under the terms of the Creative Commons Attribution License (<http://creativecommons.org/licenses/by/3.0>), which permits unrestricted use, distribution, and reproduction in any medium, provided the original work is properly cited. 

References

- [1] The Nippon Foundation-GEBCO. Seabed 2030 Project. Available from: <https://seabed2030.org/> [Accessed: June 17, 2022]
- [2] EMODnet Bathymetry Consortium: EMODnet Digital Bathymetry (DTM). 2020. DOI: <https://doi.org/10.12770/bb6a87dd-e579-4036-abe1-e649cea9881a>
- [3] International Hydrographic Organization (IHO). Guidance on Crowdsourced Bathymetry. Draft Ed 2. 2019; 51 p. Available online at: https://iho.int/iho_pubs/IHO_Download.htm
- [4] Smith WHF, Sandwell DT. Global sea floor topography from satellite altimetry and ship depth soundings. *Science*. 1997; **277**:1956-1962
- [5] Tozer B, Sandwell DT, Smith WHF, Olson C, Beale JR, Wessel P. Global bathymetry and topography at 15 arc sec: SRTM15+. *Earth and Space Science*. 2019; **6**(10):1847-1864
- [6] GEBCO Compilation Group: GEBCO 2021 Grid. 2021
- [7] Amante C, Eakins BW. ETOPO1 1 Arc-Minute Global Relief Model: Procedures, data sources and analysis. NOAA Technical Memorandum NESDIS NGDC-24. 2009
- [8] Dierssen H, Theberge A. Bathymetry: Assessing methods. In: Wang Y, editor. *Encyclopedia of Natural Resources II: Water and Air*. 1st ed. Boca Raton: Taylor & Francis Group; 2014. pp. 628-636
- [9] Smith WHF, Sandwell DT. Bathymetric prediction from dense satellite altimetry and sparse shipboard bathymetry. *Journal of Geophysical Research - Solid Earth*. 1994; **99**: 803-821
- [10] International Hydrographic Organization (IHO). IHO Data Centre for Digital Bathymetry (DCBC). 2022. Available from: <https://www.ngdc.noaa.gov/iho/> [Accessed: June 14, 2022]
- [11] Sandwell DT, Smith HF. Bathymetric estimation. In: Fu LL, Cazenave A, editors. *Satellite Altimetry and Earth Sciences*. San Diego: Academic Press; 2000. pp. 441-457. DOI: 10.1016/S0074-6142(01)80157-1
- [12] Calmant S, Baudry N. Modelling bathymetry by inverting satellite altimetry data: A review. *Marine Geophysical Researches*. 1996; **18**: 123-134. DOI: 10.1007/BF00286073
- [13] Parker RL. The rapid calculation of potential anomalies. *Geophysical Journal of the Royal Astronomical Society*. 1973; **31**:447-455. DOI: 10.1111/j.1365-246X.1973.tb06513.x
- [14] Watts AB. *Isostasy and Flexure of the Lithosphere*. Cambridge: Cambridge University Press; 2014. p. 458
- [15] Ibrahim A, Hinze WJ. Mapping buried bedrock topography with gravity. *Ground Water*. 1972; **10**(3):18-23. DOI: 10.1111/j.1745-6584.1972.tb02921.x
- [16] Kim J, Von Frese R, Lee B, Roman D, Doh SJ. Altimetry-derived gravity predictions of bathymetry by the gravity-geologic method. *Pure and Applied Geophysics*. 2011; **168**:815-826. DOI: 10.1007/s00024-010-0170-5
- [17] Hsiao YS, Cheinway H, Cheng YS, Chen LC, Hsu HJ, Tsai JS, et al. High-resolution depth and coastline over major atolls of South China Sea from satellite altimetry and imagery. *Remote Sensing of Environment*. 2016; **176**: 69-83. DOI: 10.1016/j.rse.2016.01.016

- [18] Xiang X, Wan X, Zhang R, Li Y, Sui X, Wang W. Bathymetry inversion with the gravity-geologic method: A study of long-wavelength gravity modeling based on adaptive mesh. *Marine Geodesy*. 2017;**40**:329-340. DOI: 10.1080/01490419.2017.1335257
- [19] Yeu Y, Yee JJ, Yun HS, Kim BK. Evaluation of the Accuracy of Bathymetry on the Nearshore Coastlines of Western Korea from Satellite Altimetry, Multi-Beam, and Airborne Bathymetric LiDAR. *Sensors*. 2018;**18**:2926. DOI: 10.3390/s18092926
- [20] Sun Z, Ouyang M, Guan B. Bathymetry predicting using the altimetry gravity anomalies in South China Sea. *Geodesy and Geodynamics*. 2018;**9**(2):156-161. DOI: 10.1016/j.geog.2017.07.003
- [21] DTU Space. DTU10BAT digital bathymetry model. 2022. Available from: https://www.space.dtu.dk/english/research/scientific_data_and_models [Accessed: June 14, 2022]
- [22] NOAA. ETOPO 1 digital bathymetry model. 2022. Available from: <https://www.ngdc.noaa.gov/mgg/global/> [Accessed: June 14, 2022]
- [23] GEBCO. GEBCO 2021 digital bathymetry model. 2022. Available from: <https://download.gebco.net/> [Accessed: June 14, 2022]
- [24] Scripps Institute of Oceanography. SRTM15+ v.2.3 digital bathymetry model. 2022. Available from: <https://topex.ucsd.edu/pub/archive/srtm15/> [Accessed: June 14, 2022]
- [25] Scripps Institute of Oceanography. SS v.23.1 digital bathymetry model. 2022. Available from: https://topex.ucsd.edu/pub/global_topo_1min/ [Accessed: June 14, 2022]
- [26] Andersen OB. The DTU10 Gravity field and Mean Sea surface. In: Presentation on Second International Symposium of the Gravity Field of the Earth (IGFS2). Alaska; 2010
- [27] Marks KM, Smith WHF. An evaluation of publicly available bathymetry grid. *Marine Geophysical Researches*. 2006;**27**:19-34. DOI: 10.1007/s11001-005-2095-4
- [28] Hao R, Wan X, Wang Y, Annan RF. Evaluation of four global bathymetry models by shipborne depths data. *Journal of Surveying Engineering*. 2021;**148**:2. DOI: 10.1061/(ASCE)SU.1943-5428.0000392
- [29] Abramova AS. Comparison of publicly available global bathymetry grids. In: Presentation on Gebco Fifth Science Day. Callao, Peru; 2010
- [30] Lj V. Comparison and analysis of publicly available bathymetry models in the East Adriatic Sea. *Naše more*. 2021;**2**:110-119. DOI: 10.17818/nm/2021/2.7
- [31] Sandwell DT, Muller RD, Smith WH, Garcia E, Francis R. New global marine gravity model from CryoSat-2 and Jason-1 reveals buried tectonic structure. *Science*. 2014;**346**(65):65-67. DOI: 10.1126/science.1258213
- [32] Roman DR. An Integrated Geophysical Investigation of Greenland's Tectonic History. Columbus: Ohio State University; 1999
- [33] Wei Z, Jinyun G, Zhu C, Yuan J, Chang X, Ji B. Evaluating accuracy of HY-2A/GM-derived gravity data with the gravity-geologic method to predict bathymetry. *Frontiers in Earth Science*. 2021;**9**:636246
- [34] International Hydrographic Organization (IHO). Limits of Oceans and Seas. 3rd ed. Monaco; 1953. p. 38